



Application of an Additive Self-tuning Controller for Static Synchronous Series Compensator for Damping of Sub-synchronous Resonance Oscillations

M. Abbasi, H. Shayestehkhah, B. Tousi*

Department of Electrical Engineering, Urmia University, Urmia, Iran

PAPER INFO

Paper history:

Received 27 June 2017

Received in revised form 19 September 2017

Accepted 12 December 2017

Keywords:

Static Synchronous Series Compensator

Sub-synchronous Resonance

Self-tuning

Auto Regressive Moving Average Exogenous

Recursive Least Squares

Pole Shift

ABSTRACT

In this paper, an additive self-tuning (ST) control scheme is presented for a static synchronous series compensator (SSSC) to improve performance of conventional PI control system for damping sub-synchronous resonance (SSR) oscillations. The active and reactive series compensation are provided by a three-level 24-pulse SSSC and fixed capacitor. The proposed ST controller consists of a pole shift (PS) controller and a recursive least squares (RLS). The RLS identifier algorithm is used to estimate parameters of auto regressive moving average exogenous (ARMAX) model. With this scheme, there is no any necessity for retuning the PI controller parameters under different operational circumstances of the system. The SSR analysis are performed using eigenvalue analysis, transient simulation and FFT analysis. The considered test system is adapted from IEEE First Benchmark Model. As shown in the results, the proposed additive ST controller has an effective and acceptable performance for damping of SSR under different disturbances and operating conditions. It should be noted here that all digital simulations have been done by using MATLAB.

doi: 10.5829/ije.2018.31.04a.07

1. INTRODUCTION

Series compensation is one of the economical and effective solutions to increase the power transfer capability of transmission lines and also improve transient stability [1-3]. However, this way of compensation may lead to adverse and dangerous interactions between the turbine-generator mechanical system and an electrical network which is compensated through fixed series capacitors. This phenomenon is known as sub-synchronous resonance, which can have undesirable results like shaft fatigue and possible damages or failures [4-7]. Therefore, appropriate suppression methods must be used if the initial analysis indicate that there is any possibility of SSR problems in the system [8].

The advancements of power electronic devices led to the arrival of flexible AC transmission systems (FACTS) which have attracted researcher's wide interests in recent years [9-19]. These devices can be connected in series, in parallel, or in a combination of

both. This paper focuses on the best type of series compensation controllers, the SSSC, which has been proposed by Gyugyi in 1989 [20]. The SSSC has several advantages over other series compensators [20, 21]. Beside the conventional benefits of series compensation including control of line impedance and power flow, the SSSC with a suitable damping control system can also avoid or mitigate SSR [1, 20-25].

The conventional controllers used for SSSC are mainly based on PI controllers and their designs are often based on linearized system equations under a specific operating point. Therefore, due to fixed-parameters of PI controllers, their performance degrades by changing the system operating conditions [26]. The PI controllers tuning is a challenging and complex issue, especially for a nonlinear massive power system which contains numerous switching devices [27].

In the literature [28, 29], a robust controller, sliding-mode control strategy has been proposed. However, these control methods are not self-tuned for variations in dynamics and performance of the system and their efficiency depends on the transfer function which is actually hard to find for large-scale power systems

*Corresponding Author's Email: b.tousi@urmia.ac.ir (B. Tousi)

modeled with a FACTS device [26]. Another worry is about having accurate information of all components which are needed for modeling the whole power system. By growing power systems interconnections and being more complicated, obtaining and accessing to proper and up-to-date information become really complex and approximately impossible [30].

A new method was proposed [31] for extracting the sub-synchronous frequency components through filters, in which genetic algorithm (GA) was utilized to optimize the gains of filters. However, the optimization algorithms like GA and particle swarm optimization (PSO) require evaluation function in real time uses.

In other works [32] and [33], artificial neural network (ANN) and fuzzy logic based control approaches [34] have been introduced to tune the gains of controller.

In the literature [35], the major superiorities and drawbacks of the traditional PI controller, fuzzy logic controller and ANN controller have been described. The self-tuning (ST) control technique founded on pole shift control logic has been already applied to adaptive power system stabilizers and some devices of FACTS family [30, 36].

However, in this paper, this method is used for the first time for a SSSC for damping the SSR oscillations. Here, we introduce an additive ST controller which is different from the ANN and fuzzy logic control approaches. By using proposed controller, there is no need to offline training that is rather time-consuming and essential for fuzzy logic.

The proposed method is also independent from inference rules that are fundamental for ANN control approaches. The proposed ST controller contains a PS controller and a recursive least squares (RLS) identifier. The RLS identifier algorithm is used to estimate autoregressive moving average exogenous (ARMAX) model parameters.

This paper is organized as follows: first, section II presents a brief discussion about SSSC operation and its control system. Then, section III gives a case study on SSR analysis in a series compensated system with and without SSSC. After that, in section IV, designing and performance evaluation of the additive ST control scheme are given. Finally, the conclusions of this study are reported in section V.

2. SSSC: OPERATION PRINCIPLES AND CONTROL SYSTEM

The power converter used in SSSC is commonly a multilevel and/or multi-pulse converter structure. Here, a 24-pulse three-level structure is used to model the SSSC. As we know, the control method is desirable if it

can alter the output AC voltage magnitude without affecting DC link voltage magnitude. There are two ways to achieve this goal. The first method is to use pulse width modulation (PWM) with a two-level topology which has high switching frequency and also high switching losses. The second method is to vary dead angle β with fundamental switching frequency in the three-level converter structure as elaborated elsewhere [37].

The type-I converters provide the ability of varying instantaneous values of output voltage magnitude using modulation index (k_m) and also output voltage phase angle (γ) [38]. It must be noted here that γ is about $+\pi/2$ for inductive mode and $-\pi/2$ for capacitive mode. The converter output voltage is zero for the time duration of $2\beta/\omega_0$ per half cycle. Also, by using the three-level converter scheme, the harmonic distortion is greatly reduced on the AC side [31]. The detailed three-phase model of SSSC and switching functions of the three-level 24-pulse converter is described in the literature [31].

By ignoring the output voltage's harmonics in a 24-pulse three level converter, the output voltage of phase "a" can be written as shown below:

$$V_{an}^i = \frac{8}{\pi} V_{dc} \cos(\beta) \sin(\omega_0 t + \varphi + \gamma) \quad (1)$$

V_{bn}^i and V_{cn}^i can be obtained by 120° phase shifting in succession. In addition, a specific harmonics can reach zero when the below equation is true:

$$2\beta = 180^\circ / h \quad (2)$$

where h is the number of harmonics ($h=6k\pm 1$). At $\beta_{optimum}=3.75^\circ$, the three-level 24-pulse converter treats similar to a 48-pulse converter, in which, both of 23th and 25th harmonics are negligible. In addition, the line current of phase "a" is presumed as expressed below:

$$i_a = \sqrt{(2/3)} i_a \sin(\omega t + \varphi) \quad (3)$$

2. 1. Mathematical Model of Sssc in D-Q Frame of Reference

By relinquishing the harmonics, it is possible to model the SSSC through transforming the three-phase currents and voltages to synchronous reference frame of the D-Q variables by using Kron's transformation [4, 39]. The both AC and DC sides equivalent circuits of SSSC are illustrated in Figure. 1. In Figure. 1(a), V_T is the voltage that is generated by SSSC. Also, X_r and R_r are the reactance and resistance of interfacing transformer of converter. The converter's output voltage magnitude (V^i) can be written in D-Q frame of reference as shown below:

$$V^i = \sqrt{V_D^{i^2} + V_Q^{i^2}} \quad (4)$$

where V_D^i and V_Q^i are the D and Q components of output voltage of converter which are defined as presented below:

$$V_D^i = k_m V_{dc} \sin(\varphi + \gamma) \tag{5}$$

$$V_Q^i = k_m V_{dc} \cos(\varphi + \gamma) \tag{6}$$

in which k_m is the modulation index [40] and also a function of dead angle β that can be obtained as shown below:

$$k_m = k \rho \cos \beta \tag{7}$$

where ρ is transformation ratio of interfacing transformer of SSSC. From viewpoint of the control system, it is convenient to define reactive voltage (V_R) and real voltage (V_P) as the V^i quadrature's components in phase with line current (I). V_R and V_P in terms of variables in D-Q reference frame (V_D^i and V_Q^i) are given by:

$$V_R = V_D^i \cos \phi - V_Q^i \sin \phi \tag{8}$$

$$V_P = V_D^i \sin \phi - V_Q^i \cos \phi \tag{9}$$

where, ϕ is the phase displacement of the line current with respect to Q axis. It should be noted that negative V_R indicates capacitive operation mode of SSSC and positive V_P shows that active power is absorbed by SSSC from transmission line [31].

Normalized per unit state equations of SSSC AC side can be transformed to the D-Q frame as follows:

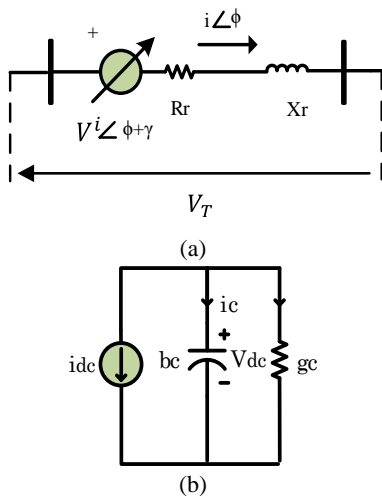


Figure 1. SSSC equivalent circuit (a) AC side and (b) DC side [15, 26]

$$\frac{d}{dt} \begin{bmatrix} i_D \\ i_Q \end{bmatrix} = \begin{bmatrix} -\frac{R_r \omega_B}{X_r} & -\omega_B & -\frac{\omega_B V_D^i}{X_r} \\ \omega_B & -\frac{R_r \omega_B}{X_r} & -\frac{\omega_B V_Q^i}{X_r} \end{bmatrix} \begin{bmatrix} i_D \\ i_Q \end{bmatrix} + \frac{\omega_B}{X_r} \begin{bmatrix} V_{TD} \\ V_{TQ} \end{bmatrix} \tag{10}$$

where I_D and I_Q are the D-Q frame components of the line current (I). The power balance equation of VSC DC and AC sides can be shown as below [38]:

$$V_{dc} I_{dc} = \frac{3}{2} (V_D^i i_D + V_Q^i i_Q) \tag{11}$$

The dynamical equation for describing DC side capacitor can be defined as follows:

$$\frac{dV_{dc}}{dt} = -\frac{\omega_b}{b_c} I_{dc} - \frac{\omega_b g_c}{b_c} V_{dc} \tag{12}$$

in which I_{dc} can be obtained as below:

$$I_{dc} = -[k_m \sin(\varphi + \gamma) I_D + k_m \cos(\varphi + \gamma) I_Q] \tag{13}$$

In Equation (12), g_c is the conductance which accounts for losses, ω_b is considered $2\pi f_{base}$ and b_c is the susceptance of dc link capacitor [37].

2. 2. Voltage Control System of SSSC The configuration of type-I controller used in SSSC is shown in Figure 2. As shown in this Figure, both magnitude (as a function of β) and phase angle of the converter output voltage (γ) are used to control real and reactive components of voltage. By controlling of V_P , the capacitor voltage (V_{dc}) is fixed at a constant value. Also, the real voltage reference V_{pref} is considered as the output of DC link voltage controller. The reactive voltage reference V_{Rref} may be kept constant. In fact, there are cases that the constant reference reactive voltage is insufficient. For this type of cases, the solution is to add a supplementary damping controller to the main control system [31]. As we know, the operating point has a significant impact on the harmonic amount of the injected voltage of SSSC. Hence, by varying the DC voltage reference, we can have the optimum harmonic performance as an outcome [37]. For three-level 24-pulse inverter, optimum harmonic performance is gained at $\beta=3.75^\circ$ where acts similar to a 48-pulse converter in steady state.

3. CASE STUDY FOR ANALYSIS OF SSR

The considered system is adapted from IEEE FBM [41]. Figure 3 presents a schematic diagram of modified IEEE FBM system which consists of a turbine, generator (modeled by a 2.2 model), excitation system,

power system stabilizer (PSS), torsional filter, transmission line with series compensation and a SSSC which only injects reactive power to the system.

The analysis of SSR is performed by considering the following primary operating conditions and presumes:

1) The generator delivers power (P_g) equal to 0.9 p.u. to the transmission line.

2) The total series compensation is kept at 0.61 p.u.

The following cases are considered for performing this study:

Case I (without SSSC): The series compensation is only provided by constant capacitor $X_{Cap1}=0.61$ p.u. and in order to accomplish the transient simulation, a small mechanical disturbance (10% step reduction in mechanical input torque) is put on at 0.5s and restored at 1s.

Case II (with SSSC): In this case, the SSSC supplies 0.16 p.u. of total series compensation ($X_{SSSC}=V_R/I$) and the rest should be provided through constant capacitor ($X_{Cap2}=0.45$ p.u.). For this case, in addition to the disturbance of the case I, a mechanical disturbance (25% step reduction in mechanical input torque) is put on at 7.5s and restored at 8s.

The data for electromechanical system, excitation system, PSS, SSSC and PI parameters have been given in the literature [37, 41].

3. 1. Eigenvalue Analysis The eigenvalue analysis method needs the linearized system equations about an operating point.

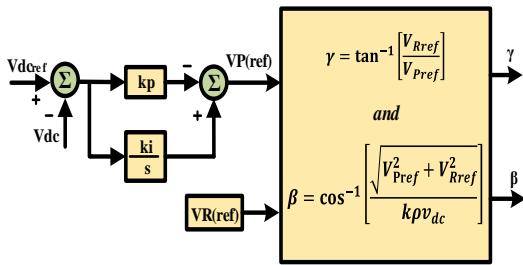


Figure 2. Type-1 controller for SSSC

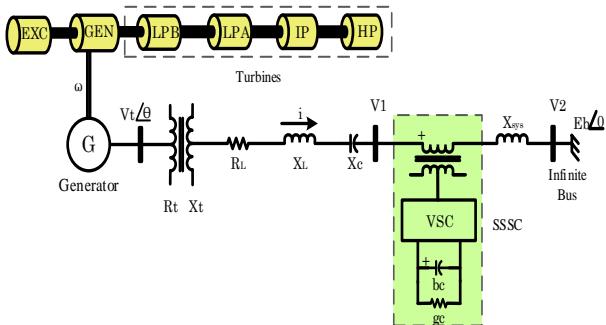


Figure 3. Modified IEEE first benchmark model with SSSC

Here, we use the approach given elsewhere [4]. The results of this methods analysis are presented in Table 1 for both of the mentioned cases. When the series compensation is set at 0.61 p.u. just by constant capacitor, the complement of the electrical resonance frequency matches with critical mode 2 of the IEEE FBM. Therefore, the system loses its stability in case I. However, at the presence of SSSC (case II), stability is shown in all of the torsional modes. The increment of network sub-synchronous mode frequency to 149.02 rad/s shows this fact that the use of SSSC in series compensation results in increasing and shifting the network resonant frequency and also reducing potential risk of the SSR problem.

3. 2. Transient Simulation

The power systems are inherently dynamical and non-linear while eigenvalue analysis, the transient simulation and FFT analysis for case I have been performed and the results are shown in Figure 4 and Figure 5. It is obvious from these figures that the values of the electrical torque and rotor angle diverge and the second mode (20.1 Hz) of FBM system is unstable. In order to evaluate the system's oscillatory modes, the FFT analysis is performed based on the IEEE FBM using MATLAB program [42].

Figure 6 depicts the FFT plot of the electrical torque in time interval of 2–14s with the time spread of 3s. It is evident from FFT analysis that the mode-2 component is dominant and decreases by time. These results are consistent with the eigenvalue analysis results. Figures 7 and 8 illustrate the results of transient simulation for case II. In the first disturbance, it is evident that the SSSC is capable of damping of SSR oscillations. However, in the second disturbance, the third mode gets excited and the system operating conditions will be changed and SSSC cannot damp the oscillations by the conventional controller which is caused by this fact that the controller parameters are adjusted for previous condition.

TABLE 1. Eigenvalues of the combined system without and with SSSC

Torsional Mode	Case I: Without SSSC	Case II: With SSSC
0	-1.8028 ± j 9.0469	-1.3185 ± j 8.2713
1	-0.2061 ± j99.449	-0.2181 ± j99.449
2	0.36965 ± j126.33	-0.0688 ± j127.01
3	-0.6468 ± j 160.42	-0.6295 ± j 160.42
4	-0.36508 ± j 202.82	-0.3645 ± j 202.82
5	-1.85041 ± j 298.17	-1.85041 ± j 298.17
Network mode (sub)	-1.622 ± j125. 4	-2.8151 ± j149.02
Network mode (super)	-2.9908 ± j 628.88	-2.8045 ± j 581.97

In other word, they are not authentic after changing the system operation condition. Also, Figure 9 shows the FFT plot of the electrical torque for case II. It is observed that in the time spans of 8–11 s and 11–14 s, the oscillations with frequency of 25.5 Hz (mode-3) begin to increase and the SSSC fails to mitigate the SSR oscillations. Consequently, for the sake of mitigating SSR under various system operating conditions, the SSSC should be equipped with an additive ST controller. This scheme maintains the functionality of the existing PI controllers. The study on the application of an additive supplementary ST control loop for SSR damping is presented at the following.

4. DESIGN AND PERFORMANCE EVALUATION OF ADDITIVE ST CONTROLLER

The principle difficulty of the SSSC control system based on conventional PI controllers was discussed in section III. As mentioned, the PI controllers cause the need to frequent tuning.

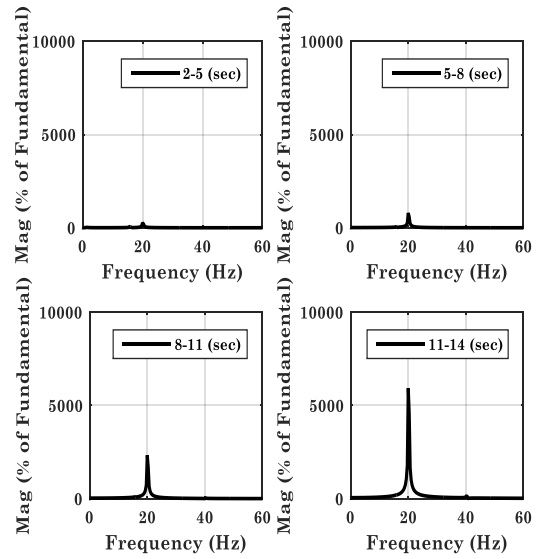


Figure 6. FFT analysis of electrical torque for case I

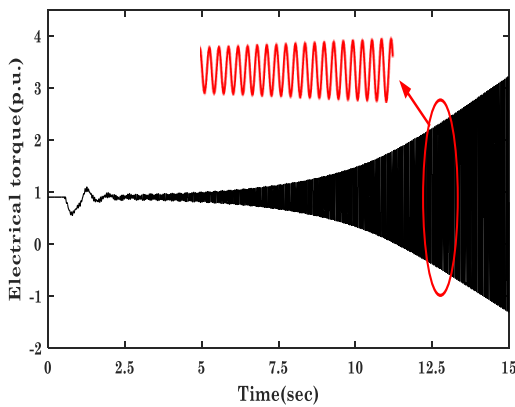


Figure 4. Variation of electrical torque in case I for 10% step decrease in mechanical input torque

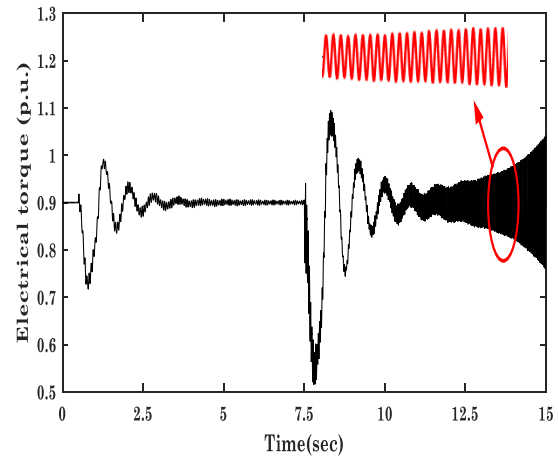


Figure 7. Variation of electrical torque in case II for 25% step decrease in mechanical input torque

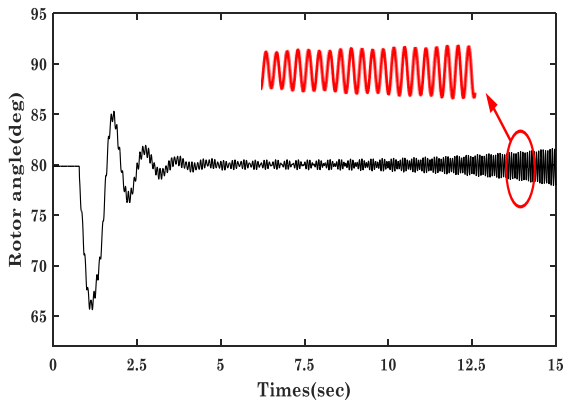


Figure 5. Variation of rotor angle in case I for 10% step decrease in mechanical input torque

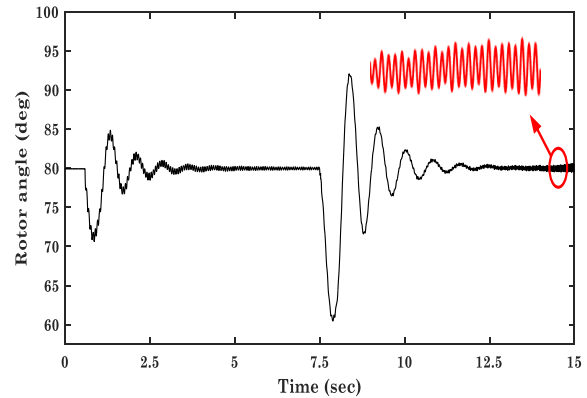


Figure 8. Variation of rotor angle in case II for 25% step decrease in mechanical input torque

Therefore, they are ineffective when SSR oscillations damping should be done under divers operating conditions. In contrast, there is no need for tuning in the proposed ST controller. This controller consists of a RLS identifier and a PS controller. The RLS identifier is assigned to the estimated model of a power system (ARMAX model) which identifies the ARMAX parameters online. Actually, the ST controllers rely on accurate identification of the ARMAX parameters. The block-diagram of the ST controller is shown in Figure 10. The measured output $y(t)$ from the power system is the electrical torque T_e while the PS controller output $u(t)$ is the supplementary damping input supplied to the control system of the SSSC for modulating the reference reactive voltage V_{ref} as shown in Figure 11.

4. 1. Armax Model At specific operating points, it is possible to utilize the ARMAX model for explaining dynamic behavior of a power system. This approach obviates the requirement for update and proper information of whole system components. The configuration of an ARMAX model can be expressed as below [43]:

$$y(t) + a_1y(t-1) + a_2y(t-2) + \dots + a_{na}y(t-na) = b_1u(t-nk) + b_2u(t-nk-1) + \dots + b_{nb}u(t-nk-nb) + e(t) + c_1e(t-1) + c_2e(t-2) + \dots + c_{nc}e(t-nc) \tag{14}$$

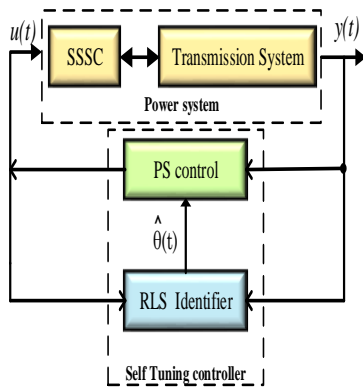


Figure 10. Overview of ST controller

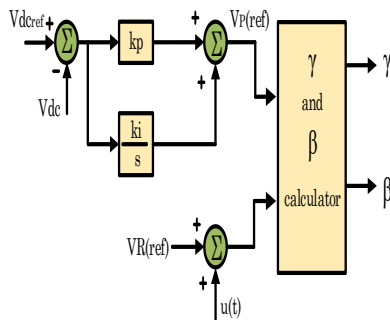


Figure 11. Overview of ST controller

where $u(t)$, $y(t)$ and $e(t)$ are the system input, system output and white noise, respectively. na is the order of AR model (number of poles); nb is the order of input model (number of zeroes plus 1); and nc is the order of MA model. In addition, nk is the number of input samples that happen before the input affects the output, also named the dead time in the system. In the z -domain, Equation (14) can be simplified as below:

$$A(z^{-1})y(t)=B(z^{-1})u(t)+C(z^{-1})e(t) \tag{15}$$

where $A(z^{-1})$, $B(z^{-1})$ and $C(z^{-1})$ are polynomials in backward shift operator z^{-1} which are defined as below [44]:

$$\begin{cases} A(z^{-1}) = 1 + a_1z^{-1} + a_2z^{-2} + \dots + a_{na}z^{-na} \\ B(z^{-1}) = b_1z^{-1} + b_2z^{-2} + \dots + b_{nb}z^{-nb} \\ C(z^{-1}) = 1 + c_1z^{-1} + c_2z^{-2} + \dots + c_{nc}z^{-nc} \end{cases} \tag{16}$$

The system modes can be identified based on the ARMAX model as the roots of characteristic polynomial as expressed below:

$$1 + a_1z^{-1} + a_2z^{-2} + \dots + a_{na}z^{-na} \tag{17}$$

4. 2. Recursive Least Squares (RLS) Among the various identification methods utilized for online estimation of parameters, the recursive least squares (RLS) algorithm has benefits like good convergence and simple calculation [45]. Based on this algorithm, the parameter vector can be presented as follows:

$$\hat{\theta}(t) = [a_1, a_2, \dots, a_{na}, b_1, b_2, \dots, b_{nb}, c_1, c_2, \dots, c_{nc}]^T \tag{18}$$

which minimizes the squares of the prediction error. The prediction error $\varepsilon(t)$ is calculated as below:

$$\varepsilon(t) = y(t) - \hat{y}(t) = e(t) \tag{19}$$

In above equation, $\hat{y}(t)$ is the prediction of $y(t)$ based on estimated parameters. The $y(t)$ can be obtained as presented below:

$$\hat{y}(t) = \psi(t)^T \hat{\theta}(t-1) \tag{20}$$

where $\psi(t)$ shows the data vector storing the last na samples of the system output and the last nb samples of the system input. The measurement variable vector ($\psi(t)$) is defined as follows:

$$\psi(t) = [-y(t-1), -y(t-2), \dots, -y(t-na), u(t-1), u(t-2), \dots, u(t-nb), \varepsilon(t-1 | \hat{\theta}(t-1)), \dots, \varepsilon(t-nc | \hat{\theta}(t-nc))]^T \tag{21}$$

The system estimated parameter vector, $\hat{\theta}(t)$ can be expressed as below:

$$\hat{\theta}(t) = \hat{\theta}(t-1) + k(t)[y(t) - \hat{y}(t)] \tag{22}$$

where $k(t)$ is the gain vector and can be obtained as:

$$k(t) = \frac{p(t-1)\psi(t)}{\lambda + \psi^T(t)p(t-1)\psi(t)} \tag{23}$$

in which λ is the forgetting factor that is utilized for discounting the significance of the older data and $p(t)$ is the covariance (of error in estimate) matrix which can be defined as below:

$$P(t) = \frac{1}{\lambda} [1 - k^T(t)\psi(t)] p(t-1) \tag{24}$$

4. 3. Pole Shift Control Once the parameters of the considered model are correctly estimated, a pole shift controller is designed for producing the desirable control signal. The considered feedback control scheme is shown in Figure 12 and the general transfer function for this controller is expressed as below:

$$\frac{u(t)}{y(t)} = -\frac{G(z^{-1})}{F(z^{-1})} \tag{25}$$

where:

$$\begin{cases} F(z^{-1}) = 1 + f_1z^{-1} + f_2z^{-2} + \dots + f_{n_f}z^{-n_f} \\ G(z^{-1}) = g_0 + g_1z^{-1} + g_2z^{-2} + \dots + g_{n_g}z^{-n_g} \end{cases} \tag{26}$$

and

$$n_f = n_b - 1 \tag{27}$$

$$n_g = n_a - 1 \tag{28}$$

The closed-loop transfer function from Figure 12 is given by:

$$H(z^{-1}) = \frac{B(z^{-1})F(z^{-1})}{A(z^{-1})F(z^{-1}) + B(z^{-1})G(z^{-1})} \tag{29}$$

Therefore the characteristic equation can be obtained as shown below:

$$T(z^{-1}) = A(z^{-1})F(z^{-1}) + B(z^{-1})G(z^{-1}) \tag{30}$$

The PS controller is based on the pole-assignment method. However, unlike the pole-assignment algorithm (in which the closed-loop poles are used to specific places), in the PS method, the characteristic equation of the open-loop system is presumed to be characteristic equation of the close-loop system and the closed-loop poles are the same open-loop poles shifted radially towards the center of the unit circle in the z - plane by a scalar factor α which is less than one [46], (in this paper $\alpha = 0.968$). Thus, the new characteristics equation

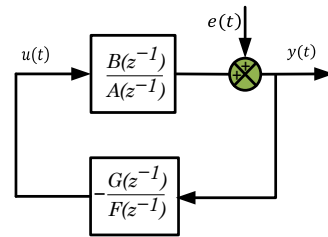


Figure 12. General feedback control scheme

can be obtained by replacing z^{-1} in $A(z^{-1})$ with αz^{-1} as follows:

$$T(z^{-1}) = A(z^{-1})F(z^{-1}) + B(z^{-1})G(z^{-1}) = A(\alpha z^{-1}) \tag{31}$$

The coefficients of polynomial in controller transfer function are obtained by comparing the coefficients on both sides of Equation (25) as follows:

$$\omega = M^{-1}.L \tag{32}$$

where L , M and ω are defined as shown below:

$$L = [(\alpha - 1)a_1 \quad (\alpha^2 - 1)a_2 \quad \dots \quad (\alpha^{n_a} - 1)a_{n_a} \quad 0 \quad \dots \quad 0]^T \tag{33}$$

$$\omega = [f_1 \quad f_2 \quad \dots \quad f_{n_f} \quad g_0 \quad g_1 \quad \dots \quad g_{n_g}]^T \tag{34}$$

$$M = \begin{bmatrix} 1 & 0 & \dots & 0 & b_1 & 0 & \dots & 0 \\ a_1 & 1 & \dots & 0 & b_2 & b_1 & \dots & 0 \\ \dots & a_1 & \dots & \dots & \dots & b_2 & \dots & \dots \\ a_{n_a} & a_{n_a-1} & \dots & 1 & b_{n_b} & b_{n_b-1} & \dots & b_1 \\ 0 & a_{n_a} & \dots & a_1 & 0 & b_{n_b} & \dots & b_2 \\ 0 & 0 & \dots & a_2 & 0 & 0 & \dots & b_3 \\ \dots & \dots & \dots & \dots & \dots & \dots & \dots & \dots \\ 0 & 0 & \dots & a_{n_a} & 0 & 0 & \dots & b_{n_b} \end{bmatrix} \tag{35}$$

in which, matrix M elements are identified by the RLS algorithm in each sampling period. The controller output can be calculated as:

$$u(t) = X^T(t).\omega = X^T(t).M^{-1}.L \tag{36}$$

where $X(t)$ is the data vector and is given by:

$$X(t) = [-u(t-1), \dots, -u(t-n_f), -y(t), -y(t-1), \dots, -y(t-n_g)]^T \tag{37}$$

4. 4. Analysis of SSR with ST Controller Here, the performance of the proposed ST controller is demonstrated for improving the damping of SSR under different system operating conditions. The transient simulation has been carried out for entire of the system including SSSC equipped with a ST controller using MATLAB-SIMULINK [27]. Both the electrical and mechanical signals can be used as the input signals of identification system. Since in practical studies, the

mechanical signals are often difficult to be measured. It should be noted that the generator electrical torque is used for parameter identification and computation of control signal. It should be noted that, the sampling time of 0.005s (200Hz) has been chosen for the identifier and the control output is limited between u_{min} and u_{max} . Also, system order and forgetting factor are considered 50 and 0.9998, respectively, such as [47]. For proving the accurate performance of identifier in tracking of the system behavior under various operating points and disturbances, two different disturbances (similar to case II in section III) are considered. In Figure 13, output of the RLS identifier at different operating conditions is shown, in which, it is evident that after the occurring of disturbances in the system, the convergence of the identified parameters is fast and accurate.

The comparison of variation of electrical torque and rotor angle is shown in Figures 14 and 15, respectively. It is observed that performance of the PI controller designed for a specific operating point, degrades with changing the operating condition and in some cases the system may even become unstable.

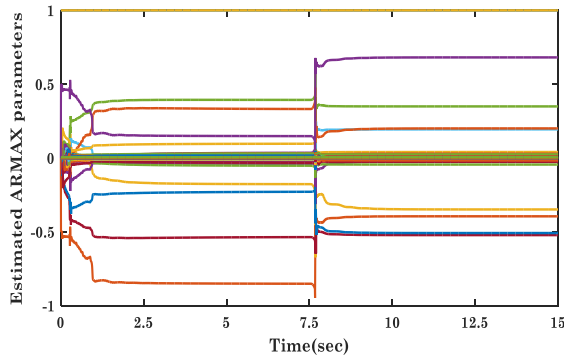


Figure 13. Excursions in ARMAX parameters following two different disturbances with RLS identifier

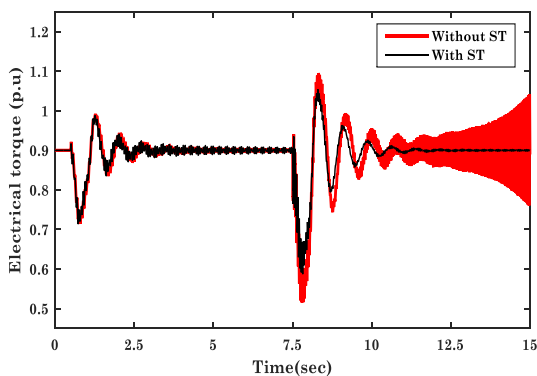


Figure 14. Variation of electrical torque for 10 and 25% step decrease in mechanical input torque with ST controller

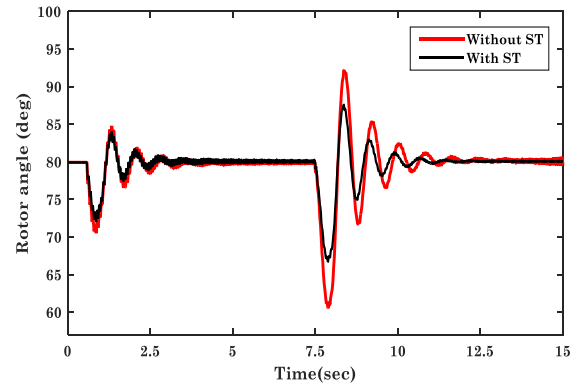


Figure 15. Variation of rotor angle for 10 and 25% step decrease in mechanical input torque with ST controller

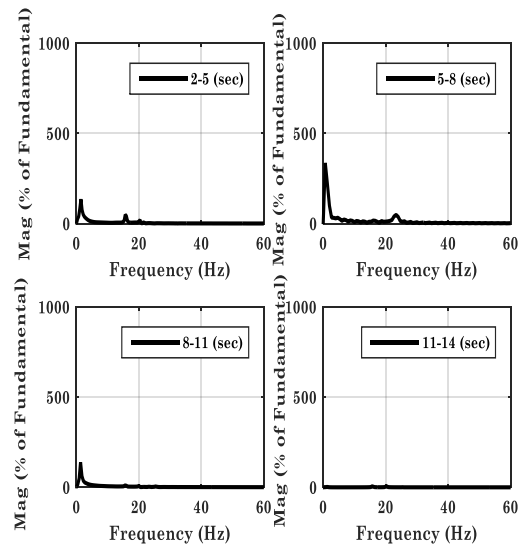


Figure 16. FFT analysis of electrical torque for 10 and 25% step decrease in mechanical input torque with ST controller

Also, as shown in Figure 16, the results of FFT analysis of the electrical torque obviously indicate that the ST controller is effective in damping oscillatory modes. According to Figures 14, 15 and 16, the effectiveness and robustness of the proposed additive ST controller for damping SSR oscillations are validated. When a disturbance happens in system, the ST controller is able to track the changes of the system operating conditions and also inject a proper signal to increase the damping of the unstable modes. In addition, in using the proposed ST controller, the overshoot and the settling times are less than the PI controller's.

5. CONCLUSION

Based on eigenvalue analysis, transient simulation and FFT analysis, it has been shown in this paper that

presence of SSSC decreases the risk of SSR. However, the SSSC without ST control loop isn't SSR neutral. Therefore, a supplementary ST controller for improving performance of the conventional PI controllers in damping sub-synchronous resonance oscillations has been designed and tested on a system adapted from IEEE First Benchmark Model.

The design of a ST controller does not require the proper and update information of all the system components and this approach is based on measurement. Accurate and fast convergence of identified parameters ensures favorable performance, even during large disturbances with the fixed PS factor, which have been verified by time-domain simulations and eigenvalue analysis. The proposed controller can be applied for other FACTS devices without the need to retune the parameters. Also, because of the use of online identification, the proposed controller has the ability of adapting to divers operating conditions and new configurations of the system. Finally, it is evident from simulation results that SSSC using add-on ST controller can damp the sub-synchronous oscillations quickly and better than the conventional PI controllers.

6. REFERENCES

- Padiyar, K., "Facts controllers in power transmission and distribution", (2007).
- Lim, J.U. and Moon, S.I., "An analytical approach for the operation of series compensators to relieve power flow congestion", *International Transactions on Electrical Energy Systems*, Vol. 13, No. 4, (2003), 247-252.
- Bera, P., Das, D. and Basu, T., "Tuning of excitation and tsc-based stabilizers for multimachine power system", *International Journal of Engineering, Transactions B: Applications*, Vol. 23, No. 1, (2010), 37-52.
- Padiyar, K., "Analysis of subsynchronous resonance in power systems, Springer Science & Business Media, (2012).
- Anderson, P.M., Agrawal, B.L. and Van Ness, J.E., "Subsynchronous resonance in power systems, John Wiley & Sons, Vol. 9, (1999).
- Kundur, P., Balu, N.J. and Lauby, M.G., "Power system stability and control, McGraw-hill New York, Vol. 7, (1994).
- Salehi, M. and Davarani, R.Z., "Effect of different turbine-generator shaft models on the subsynchronous resonance phenomenon in the double cage induction generator based wind farm", *International Journal of Engineering-Transactions B: Applications*, Vol. 29, No. 8, (2016), 1103-1111.
- group, I.S.w., "Countermeasures to subsynchronous resonance problems", *Trans. on Power Apatatus and Systems*, Vol. 99, No. 5, (1980), 168-175.
- Han, B.M. and Ledwich, G., "Dynamic performance analysis of novel unified power flow controller with computer simulation and scaled-model experiment", *International Transactions on Electrical Energy Systems*, Vol. 18, No. 3, (2008), 250-265.
- Xiao, Y. and Song, Y., "Power flow studies of a large practical power network with embedded facts devices using improved optimal multiplier newton-raphson method", *International Transactions on Electrical Energy Systems*, Vol. 11, No. 4, (2001), 247-256.
- Amrane, Y., Boudour, M. and Belazzoug, M., "A new hybrid technique for power systems multi-facts optimization design", *International Transactions on Electrical Energy Systems*, Vol. 25, No. 11, (2015), 2961-2981.
- Chong, B., Zhang, X., Godfrey, K., Yao, L. and Bazargan, M., "Optimal location of unified power flow controller for congestion management", *International Transactions on Electrical Energy Systems*, Vol. 20, No. 5, (2010), 600-610.
- Singh, J., Tripathy, P., Singh, S. and Srivastava, S., "Development of a fuzzy rule based generalized unified power flow controller", *International Transactions on Electrical Energy Systems*, Vol. 19, No. 5, (2009), 702-717.
- Mohammadalizadeh-Shabestary, M., Hashemi-Dezaki, H., Mortazavian, S., Askarian-Abyaneh, H. and Gharehpetian, G., "A general approach for optimal allocation of facts devices using equivalent impedance models of vscs", *International Transactions on Electrical Energy Systems*, Vol. 25, No. 7, (2015), 1187-1203.
- Song, Y. and Liu, J., "Steady-state power flow and voltage control by unified power-flow controllers, part 1: Modelling and algorithms", *International Transactions on Electrical Energy Systems*, Vol. 10, No. 1, (2000), 53-57.
- Khederzadeh, M. and Ghorbani, A., "Statcom modeling impacts on performance evaluation of distance protection of transmission lines", *International Transactions on Electrical Energy Systems*, Vol. 21, No. 8, (2011), 2063-2079.
- Zafari, A. and Jazaeri, M., "Statcom systems in distribution and transmission system applications: A review of power-stage topologies and control methods", *International Transactions on Electrical Energy Systems*, Vol. 26, No. 2, (2016), 323-346.
- Kasztenny, B., Hatziaodniu, C. and Funk, A., "Vsi-based series compensation scheme for transmission lines", *International Transactions on Electrical Energy Systems*, Vol. 9, No. 2, (1999), 101-108.
- Deepa, S., Babu, S.R. and Ranjani, M., "A robust statcom controller using particle swarm optimization", *International Journal of Engineering-Transactions B: Applications*, Vol. 27, No. 5, (2013), 731-738.
- Hingoranl, N.G. and Gyugyi, L., "Understanding facts", *A John Wiley & Sons, Inc., Publication*, (2000).
- Pillai, G., Ghosh, A. and Joshi, A., "Torsional interaction studies on a power system compensated by sssc and fixed capacitor", *IEEE transactions on power delivery*, Vol. 18, No. 3, (2003), 988-993.

22. Jamila, E. and Abdelmjid, S., "Comparative study of the performance of static synchronous compensator, series compensator and compensator/battery integrated to a fixed wind turbine", Vol. 29, No. 4, (2016), 581-589.
23. Nagarajan, S.T. and Kumar, N., "Fuzzy logic control of svcs for damping ssr in series compensated power system", *International Transactions on Electrical Energy Systems*, Vol. 25, No. 9, (2015), 1860-1874.
24. Khazaie, J., Mokhtari, M., Badkubi, S., Khalilian, M. and Nazarpour, D., "Sub-synchronous resonance mitigation via distributed power flow controller", *International Transactions on Electrical Energy Systems*, Vol. 23, No. 6, (2013), 751-766.
25. Xie, X., Jiang, Q. and Han, Y., "Damping multimodal subsynchronous resonance using a static var compensator controller optimized by genetic algorithm and simulated annealing", *International Transactions on Electrical Energy Systems*, Vol. 22, No. 8, (2012), 1191-1204.
26. Malhotra, U. and Gokaraju, R., "An add-on self-tuning control system for a upfc application", *IEEE Transactions on Industrial Electronics*, Vol. 61, No. 5, (2014), 2378-2388.
27. Mitra, P. and Venayagamoorthy, G.K., "An adaptive control strategy for dstatcom applications in an electric ship power system", *IEEE Transactions on power electronics*, Vol. 25, No. 1, (2010), 95-104.
28. Loukianov, A.G., Cañedo, J.M., Fridman, L.M. and Soto-Cota, A., "High-order block sliding-mode controller for a synchronous generator with an exciter system", *IEEE Transactions on Industrial Electronics*, Vol. 58, No. 1, (2011), 337-347.
29. Mi, Y., Fu, Y., Wang, C. and Wang, P., "Decentralized sliding mode load frequency control for multi-area power systems", *IEEE Transactions on Power Systems*, Vol. 28, No. 4, (2013), 4301-4309.
30. Domahidi, A., Chaudhuri, B., Korba, P., Majumder, R. and Green, T.C., "Self-tuning flexible ac transmission system controllers for power oscillation damping: A case study in real time", *IET generation, transmission & distribution*, Vol. 3, No. 12, (2009), 1079-1089.
31. Thirumalaivasan, R., Janaki, M. and Prabhu, N., "Damping of ssr using subsynchronous current suppressor with sssc", *IEEE Transactions on Power Systems*, Vol. 28, No. 1, (2013), 64-74.
32. Chang, C.-T. and Hsu, Y.-Y., "Design of an ann tuned adaptive upfc supplementary damping controller for power system dynamic performance enhancement", *Electric Power Systems Research*, Vol. 66, No. 3, (2003), 259-265.
33. Qiao, W. and Harley, R.G., "Indirect adaptive external neuro-control for a series capacitive reactance compensator based on a voltage source pwm converter in damping power oscillations", *IEEE Transactions on Industrial Electronics*, Vol. 54, No. 1, (2007), 77-85.
34. Duan, X.-G., Deng, H. and Li, H.-X., "A saturation-based tuning method for fuzzy pid controller", *IEEE Transactions on Industrial Electronics*, Vol. 60, No. 11, (2013), 5177-5185.
35. Liu, C.-H. and Hsu, Y.-Y., "Design of a self-tuning pi controller for a statcom using particle swarm optimization", *IEEE Transactions on Industrial Electronics*, Vol. 57, No. 2, (2010), 702-715.
36. Ramakrishna, G. and Malik, O., "Radial basis function identifier and pole-shifting controller for power system stabilizer application", *IEEE Transactions on Energy Conversion*, Vol. 19, No. 4, (2004), 663-670.
37. Padiyar, K. and Prabhu, N., "Analysis of subsynchronous resonance with three level twelve-pulse vsc based sssc", in TENCON 2003. Conference on Convergent Technologies for the Asia-Pacific Region, IEEE. Vol. 1, (2003), 76-80.
38. Schauder, C. and Mehta, H.n., "Vector analysis and control of advanced static var compensators", in IEE Proceedings C (Generation, Transmission and Distribution), IET. Vol. 140, (1993), 299-306.
39. Padiyar, K.R., "Power system dynamics—stability and control", (2002).
40. Kumar, L.S. and Ghosh, A., "Modeling and control design of a static synchronous series compensator", *IEEE transactions on power delivery*, Vol. 14, No. 4, (1999), 1448-1453.
41. group, I.S.w., "First benchmark model for computer simulation of subsynchronous resonance", *IEEE transactions on power apparatus and systems*, Vol. 96, No. 5, (1977), 1565-1572.
42. Matlab, U.s.G., *Natick, ma: The math works*. 1994, Inc.
43. Liung, L., "System identification-theory for the user 2nd ed", *PTR Prentice Hall, Upper Saddle River, NJ*, (1999).
44. Zhou, N., Trudnowski, D.J., Pierre, J.W. and Mittelstadt, W.A., "Electromechanical mode online estimation using regularized robust rls methods", *IEEE Transactions on Power Systems*, Vol. 23, No. 4, (2008), 1670-1680.
45. Astrom, K. and Wittenmark, B., *Adaptive control. Mineola*. 2008, New York: Dover Publications, Inc.
46. Chen, G.-P., Malik, O., Hope, G., Qin, Y.-H. and Xu, G.-Y., "An adaptive power system stabilizer based on the self-optimizing pole shifting control strategy", *IEEE Transactions on Energy Conversion*, Vol. 8, No. 4, (1993), 639-645.
47. Khalilinia, H. and Venkatasubramanian, V., "Subsynchronous resonance monitoring using ambient high speed sensor data", *IEEE Transactions on Power Systems*, Vol. 31, No. 2, (2016), 1073-1083.

Application of an Additive Self-tuning Controller for Static Synchronous Series Compensator for Damping of Sub-synchronous Resonance Oscillations

M. Abbasi, H. Shayestehkhah, B. Tousi

Department of Electrical Engineering , Urmia University, Urmia, Iran

PAPER INFO

چکیده

Paper history:

Received 27 June 2017

Received in revised form 19 September 2017

Accepted 12 December 2017

Keywords:

Static Synchronous Series Compensator

Sub-synchronous Resonance

Self-tuning

Auto Regressive Moving Average Exogenous

Recursive Least Squares

Pole Shift

در این مقاله، یک کنترل کننده خود تنظیم برای یک جبران ساز سنکرون سری اساتیکی (SSSC) ارائه می گردد که هدف از آن بهبود عملکرد سیستم کنترل PI مرسوم در کاهش میراسازی نوسانات تشدید زیر سنکرون (SSR) می باشد. جبران سازی سری اکتیو و راکتیو به ترتیب توسط یک SSSC سه سطحه 24 پالس و یک خازن ثابت انجام می گیرد. سیستم کنترلی پیشنهادی متشکل از یک کنترل کننده شیفت قطب (PS) و حداقل مربعات بازگشتی (RLS) می باشد. الگوریتم شناسایی RLS برای تخمین پارامترهای مدل ARMAX مورد استفاده در این مطالعه به کار رفته است. بر اساس طرح پیشنهادی، نیازی برای تنظیم مجدد پارامترهای کنترل کننده PI تحت شرایط مختلف کاری سیستم وجود نخواهد داشت. تحلیل های SSR با استفاده از آنالیز مقادیر ویژه، شبیه سازی حالت گذرا و آنالیز FFT انجام گرفته اند. همانطور که نتایج این مطالعه بر روی مدل اول محک IEEE به وضوح نشان داده اند، کنترل کننده خود تنظیم پیشنهادی در جهت میراسازی نوسانات تشدید زیر سنکرون دارای عملکرد قابل قبول و موثری تحت اختلالات و شرایط کاری مختلف سیستم می باشد. لازم به ذکر است که تمام شبیه سازی ها توسط نرم افزار MATLAB انجام شده اند.

doi: 10.5829/ije.2018.31.04a.07